son, P., Eds.; Ann Arbor Science: Ann Arbor, MI 1983; pp 159-171.
(9) Anderson, F. E.; Prausnitz, J. M. Inhibition of Gas Hydrates by Methanol. *AIChE J.* **1986**, *32*, 1321.
(10) Techne Incorporated. Tecam Temperature Calibration Baths, Catalog no. 301/302, Princeton, NJ, 1982.
(11) Dimitrelis, D. Phase Equilibria for Supercritical Fluid Extraction. Doctoral Dissertation, University of California, Berkeley, CA, 1989.
(12) *Anthracene and Phenanthrene*; API Monograph Series; API Publication 708; American Petroleum Institute: Washington, DC, 1979.
(13) Cotterman, R. L.; Schwartz, B. J.; Prausnitz, J. M. Molecular Thermodynamics for Fluids at Low and High Densities. Part I: Pure Fluids Containing Small or Large Molecules. *AIChE J.* **1986**, *32*, 1787.
(14) Cotterman, R. L.; Prausnitz, J. M. Molecular Thermodynamics for Fluids at Low and High Densities. Part II: Phase Equilibria for Mixtures Containing Components with Large Differences in Molecular Size or Potential Energy. *AIChE J.* **1986**, *32*, 1799.
(15) Kohn, J. P.; Luks, K. D.; Kulkarni, A. J. Solubility of Hydrocarbons in Cryogenic NGL and LNG. *Proceedings of the Fifty-Third Annual Convention*; Gas Processors Association: Tulsa, OK, 1974; pp 21-25.
(16) Ng, S.; Harris, H. G.; Prausnitz, J. M. Henry's Constants for Methane, Ethane, Ethylene, Propane, and Propylene in Octadecane, Eicosane, and Docosane. *J. Chem. Eng. Data* **1969**, *14*, 482.
(17) McMakin, I. E., Jr.; van Winkle, M. Vapor-Liquid Equilibrium of *n*-Hexadecane-Bibenzyl-Phenanthrene System at 100 mm of Mercury Absolute. *J. Chem. Eng. Data* **1962**, *7*, 9.
(18) Tietz, M.; Dimitrelis, D.; Prausnitz, J. M. The Effect of an Aqueous Entrainer on Phase Equilibria for Supercritical Extraction of Heavy Fossel Fuels with Propane. Report 22471; Lawrence Berkeley Laboratory, University of California: Berkeley, CA, November, 1986.

Received for review July 11, 1988. Accepted January 27, 1989. This work was supported by the Director, Office of Energy Research, Office of Basic Energy Sciences, Chemical Sciences Division of the U.S. Department of Energy under Contract No. DE-AC03-76SF00098. For additional financial support we are also grateful to Exxon Research and Engineering Company, to the donors of the Petroleum Research Fund, administered by the American Chemical Society, and to the National Science Foundation.

High-Pressure Vapor–Liquid Equilibria Involving Mixtures of Nitrogen, Carbon Dioxide, and *n*-Butane

Steven K. Shibata[†] and Stanley I. Sandler*

Department of Chemical Engineering, University of Delaware, Newark, Delaware 19716

A new high-pressure vapor–liquid equilibrium apparatus has been constructed with the capability of measuring the compositions and densities of the coexisting equilibrium phases at constant temperature and/or pressure. This apparatus was tested with the carbon dioxide + *n*-butane system with excellent agreement observed between our results and previously published data. Data are also reported for the nitrogen + *n*-butane system and the previously unmeasured nitrogen + carbon dioxide + *n*-butane system. These data were modeled with the Peng–Robinson equation of state. Excellent fits were obtained for the compositions in the carbon dioxide + *n*-butane system, but a poor fit was obtained for the nitrogen + *n*-butane data. The ability of the Peng–Robinson equation of state to accurately predict the phase behavior of the ternary mixture is dependent on the fits of the binary data, and therefore the ternary data are also not fit well. In all cases the liquid densities are poorly predicted with the Peng–Robinson equation of state.

Introduction

Petroleum reservoir management, enhanced oil recovery, and separation processes in the oil and gas industries all involve modeling phase behavior of multicomponent mixtures consisting of hydrocarbons, carbon dioxide, nitrogen, and other nonhydrocarbons. The motivation for this research is to obtain experimental data on these systems and to utilize these data in evaluating equations of state and their mixing rules. By simultaneously determining both the compositions and the densities of the coexisting phases, equations of states and their mixing rules can be more stringently tested than with composition data alone. In addition, correlations of the binary data are used to predict our ternary data to test the premise that the behavior of multicomponent systems can be accurately predicted from data for binary systems.

[†] Present address: E. I. du Pont de Nemours & Company, Technical Group, Seaford, DE 19973.
* Author to whom correspondence should be addressed.

Equipment

The new apparatus is a double-recirculation cell with a maximum temperature and pressure of 300 °F and 5000 psia, respectively. The key components of the apparatus are a visual cell, recirculation pumps, and the density meters. As shown in Figure 1, the center of the apparatus is a 100-cm^3 through-windowed cell manufactured by Ruska. This cell has ports in the side, top, and bottom. Modified Ruska fittings in the top and bottom ports allow a countercurrent flow configuration in the cell with the liquid pouring into the vapor and the vapor bubbling up through the liquid. The side port is used for temperature measurement.

Recirculation is the result of two magnetic pumps (*1*); each pump is driven mechanically with ring magnets surrounding the barrel containing the piston. The magnets are supported within a carriage assembly attached to a small steel cable, which passes through the roof of the oven. No thermal disturbances were created by this arrangement since the motors driving the cables are located outside of the controlled temperature bath.

The last major component in the equipment is the Mettler Paar vibrating-tube density meters. The density meters consist of a digital readout box [DMA 60] and two vibrating-tube assemblies [DMA 512], one for each recirculation loop. For our application, the vibrating tube and the stabilizing block were separated from the sensitive electronics, because the electronics could not withstand the temperatures to which the vibrating tubes were subject. Calibration runs for each tube were made with an evacuated tube and a tube filled with distilled water, since this range of the calibration points bracketed all experimental densities. These density calibration constants are temperature dependent and therefore were determined at each temperature of interest and were checked periodically.

A double-recirculation, countercurrent flow configuration was used since this choice allowed measuring the phase densities of the recirculating phases. The schematic diagram of the apparatus is shown in Figure 1. Each recirculation loop contains a density tube, magnetic recirculation pump, and a set of sampling valves. Constant temperatures are maintained by enclosing the entire system in a Blue M oven [POM7-136C-3]. We operated the oven under manual control so as to minimize

0021-9568/89/1734-0291$01.50/0

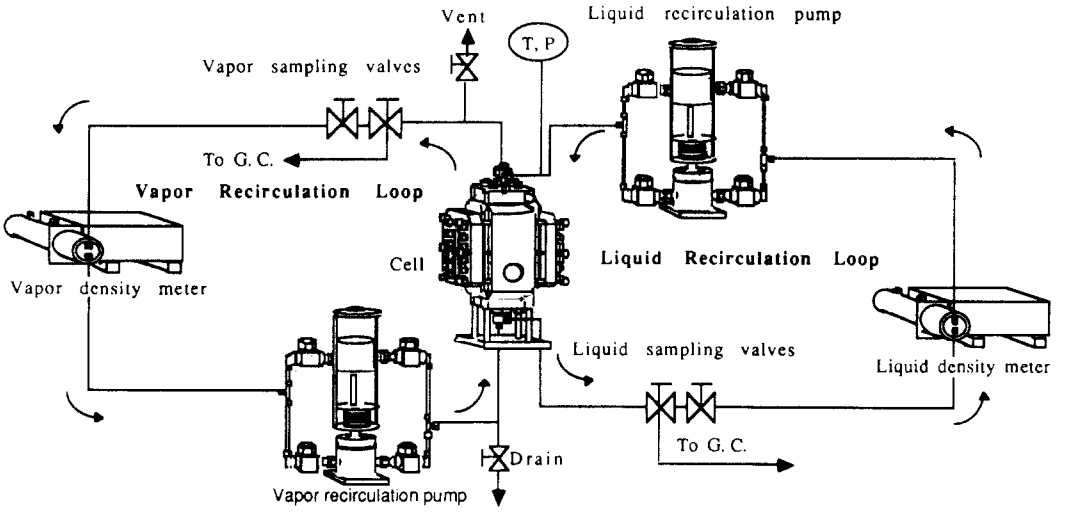

Figure 1. Flow configuration of the apparatus. This equipment is designed as a double-recirculation unit with both the liquid and vapor phases recirculating. With the excellent mixing achieved in the cell, equilibrium is often reached within an hour or less. Within each recirculation loop is a set of sampling valves, a vibrating-tube density meter, and a magnetic recirculation pump.

cell temperature fluctuations to within a tenth of a degree during an experimental run.

To prevent the potential exposure of flammable chemicals to the oven heaters, an aluminum box encloses the entire apparatus in the oven. Nitrogen is constantly purged through the box to prevent a buildup of hazardous material should a leak occur. A rotameter is used to monitor the amount of nitrogen flowing through the box. System temperatures are monitored by five type E thermocouples located in the cell, liquid recirculation loop, vapor recirculation loop, oven, and the nitrogen box. Although only the cell temperatures are reported, the other four were used as indicators of temperature fluctuations in system. Since the cell is a large block of metal, it is the slowest to respond to any temperature excursions. The thermocouples are referenced to 0 °C through cold junctions maintained in an ice bath. The millivolt readings are measured in a Biddle millivolt potentiometer [72-3110]. This unit was calibrated with a Fluke multimeter [8520A] connected to a platinum resistance thermometer. Errors in the calibration procedure are estimated to be ±0.05 °C.

System pressures are measured with a Budenberg dead-weight tester [380H] coupled with a Ruska differential pressure transducer and differential pressure null indicator [2413-705]. Accuracy is 0.1 psi up to 800 psig and 2 psi above 800 psig. Preliminary pressure readings are made with a 0–5000 psia Heise dial gauge, to speed up the determination of the exact pressure with the dead-weight tester.

The gaseous components are generally fed into the apparatus directly from their cylinders. Grade 5 nitrogen, instrument grade carbon dioxide, and instrument grade *n*-butane were used as received. For pressures above cylinder pressure or for feeding liquid components, either a Milton Roy minipump [396] (condensed vapors or liquids), or the High Pressure Equipment pressure generator [62-6-10] (gases) are used. Both of these can produce pressures up to the maximum of the apparatus. All feed enters the apparatus through the vapor sampling line.

After all components have been fed into the cell and the apparatus is at the desired temperature and pressure, a run begins. Both liquid and vapor streams are recirculated using the magnetic pumps for a period of 30 to 45 min. During this time, at intervals of 15 min, the recirculation is stopped for density measurements. Once the cell temperature and vapor and liquid densities have stabilized, the recirculation pumps are shut off, and the settling period begins. [*Note*: A longer recirculation period may be necessary if the system is not thermally equilibrated initially or the system is near the mixture critical point.] The purpose of the settling period is 2-fold. First, some time is needed to ensure complete separation of the phases in the cell, and second, the phase densities are best measured with the recirculation pumps off. Although the magnetic pumps are double-acting, the flow is not completely pulseless, so that the densities fluctuate somewhat while the pumps are on. The settling period usually lasts approximately 30 min, at which time the system pressure is determined with the dead-weight tester.

With the two phases separated and the phase densities, cell temperature, and cell pressure recorded, the system is ready for sampling. The sampling period consists of three intervals, trapping, mixing, and injecting, with the entire process lasting approximately 2–3 h. Sampling is initiated by evacuating the liquid and vapor sample bombs connected to the capillary sample lines. Small pressure gauges attached to the sample bombs indicate when evacuation is complete.

Although the sampling valves are located in the recirculation loops, we follow two procedures to ensure that representative samples are taken from the Ruska cell. The apparatus was built with the sampling valves located as close as possible to the cell, with each sample valve located between the cell and another valve. Closing this second valve seals off the recirculation loop from the sample valve so that samples are taken only from the Ruska cell. Also, we first purge the lines between the cell and the sample valves. After the purged material has been evacuated, the sampling system is isolated from the vacuum pump, and we are ready to sample. Vapor samples are taken first; however, no significant differences were noted when liquid samples were removed first.

Monitoring sample bomb pressures is crucial, as two phases can form in the bombs. Approximate dew point pressure calculations were made using a cubic equation of state for a wide range of compositions, and the lowest calculated pressure set the upper limit for the sampling pressure, which was carefully monitored by the small pressure gauges attached to the bombs. Additonally, the sample bombs and transfer lines were heated to prevent any condensation.

The vapor samples were trapped by slowly opening the valve connecting the sample bomb to the system. After the sample bomb reached the predesignated pressure (usually about 12 psia), the sample valve was shut. However, the sample bomb valve was left open for 30 min to allow ample time for samples to travel through several feet of capillary tubing into the sample

bombs. Immediately after the vapor sample was collected, the liquid sample was taken.

Small pressure drops during sampling are inevitable, since the system is not a variable-volume apparatus. A 2–4 psi pressure drop accompanies the removal of a liquid sample and a 3–6 psi drop results from the vapor sample removal. These pressure drops appear to have minimal effect on the compositions as on numerous occasions second samples of each phase have been removed from the system, and these were in excellent agreement with the initial samples.

After the trapping period was completed, the valves to the sample bombs were closed, and 20–30 min was allowed for the samples to equilibrate before injection into the gas chromatograph (GC). Next, the sample bomb was disconnected from the sample line and connected to the GC inlet box. This box is connected to a 0–600-kPa digital Heise gauge, the vacuum system, and a pneumatic sampling valve. After the GC inlet box was completely evacuated, the pressure gauge line and the vacuum lines were closed, and a sample was introduced into the inlet box and then into an Antek 300 gas chromatograph with a thermal-conductivity detector and 6-ft Porapak Q columns for analysis. For the binary mixtures studied, separation of the components was relatively simple with the GC operating in the isothermal mode. Temperature programming was required to separate the nitrogen and carbon dioxide peaks in the ternary mixtures while still desorbing the *n*-butane in a reasonable period of time. The oven temperature was maintained at 125 °C to separate the nitrogen and carbon dioxide peaks and then ramped at 20 °C/min to 150–200 °C for the *n*-butane peak.

The integrator used was a Spectra-Physics minigrator [21947-010]. Generally, three sample injections were performed for each sample analysis. The area fraction results of the three injections usually led to a standard deviation of 3.0×10^{-3} in mole fraction. Systematically varying area fractions or large standard deviations among the samples resulted in another sample being taken from the cell. The calibration of the gas chromatograph was performed by analyzing several specially prepared gaseous mixtures of known composition selected to span the entire range of expected experimental compositions. These mole fraction–area fraction data were then fit with a Redlich–Kister expansion and a calibration curve was determined. The gas mixtures utilized in the calibration were prepared in the apparatus constructed by Eckert (*2*), except that a small mixing impeller was added to each 1-L bomb.

For the binary mixtures, the data were collected isothermally, as sets of vapor- and liquid-phase compositions and densities at various pressures. Each isotherm begins with the measurement of the heavy-component vapor pressure and ends with measurements near the mixture critical point, usually with vapor and liquid mole fractions within 0.1 of each other. Sampling close to the critical point is difficult as the phase separation becomes less distinct and pressure drops associated with sampling perturb the equilibrium. All binary systems were studied by measuring VLE data at equally spaced pressure intervals of 200 or 500 psi, up to near critical conditions where more points were measured to document the rapidly changing phase behavior.

The ternary data were taken at constant temperature and pressure. Thus, each ternary data set consists of two isotherms with measurements along three to five isobars at each temperature and a wide range of compositions at each value of T and P. Generally, 7 liquid composition points were measured at each pressure, resulting in 25–30 data points at each temperature.

Measurement of a ternary data set begins with the equilibration of the apparatus to the desired temperature. The heaviest component (no. 3) is added first and the lightest component (no. 1) is added next until the desired pressure is reached. [If the component with middle volatility were added second, the binary mixture may exist as a one-phase mixture at the higher operating pressures.] Equilibration and sampling proceeds as with binary mixtures. Advancing from one point to the next at constant pressure requires removal of some vapor and addition of the second component to return the system to the original pressure. The vapor phase rather than the liquid phase is removed, because the majority of the light component is contained in that phase. Collection of a data set proceeds until either most of the first component is removed so that the other binary system is approached (a mixture of the second and third component) or a mixture critical point is reached.

Table I. Vapor–Liquid Equilibrium Data for the 310.9 K (37.7 °C) Isotherm of the Carbon Dioxide + *n*-Butane Binary System

T, K	P, bar	x_{CO_2}	y_{CO_2}	ρ_L, g/cm^3	ρ_V, g/cm^3
310.7	3.56	0.0000	0.0000	0.5562	0.0106
310.9	6.98	0.0347	0.4608	0.5577	0.0143
310.8	13.90	0.1169	0.7176	0.5658	0.0281
311.1	20.54	0.1963	0.7959	0.5757	0.0432
310.8	27.55	0.2924	0.8409	0.5845	0.0594
310.9	34.53	0.3878	0.8679	0.5962	0.0788
311.0	41.50	0.4911	0.8859	0.6071	0.1005
310.9	48.64	0.6005	0.9010	0.6176	0.1280
310.8	55.57	0.7075	0.9138	0.6224	0.1573
310.9	61.97	0.7943	0.9240	0.6184	0.1955
310.8	68.93	0.8772	0.9351	0.5902	0.2552
311.1	72.31	0.9085	0.9389	0.5390	0.3144
310.9	73.96	0.9214	0.9341	0.4649	0.3611

Table II. Vapor–Liquid Equilibrium Data for the 344.3 K (71.1 °C) Isotherm of the Carbon Dioxide + *n*-Butane Binary System

T, K	P, bar	x_{CO_2}	y_{CO_2}	ρ_L, g/cm^3	ρ_V, g/cm^3
344.3	8.35	0.0000	0.0000	0.5130	0.0216
344.3	10.50	0.0177	0.1748	0.5152	0.0252
344.3	15.65	0.0604	0.4077	0.5180	0.0349
344.3	20.61	0.1032	0.5355	0.5202	0.0450
344.2	27.59	0.1637	0.6290	0.5229	0.0621
344.3	34.49	0.2250	0.6909	0.5249	0.0764
344.2	41.49	0.2894	0.7266	0.5261	0.0938
344.3	48.37	0.3550	0.7529	0.5263	0.1161
344.3	54.98	0.4154	0.7653	0.5249	0.1377
344.3	62.11	0.4919	0.7816	0.5192	0.1652
344.3	69.00	0.5625	0.7904	0.5089	0.1982
344.2	76.03	0.6322	0.7841	0.4813	0.2486
344.2	79.61	0.6615	0.7679	0.4452	0.2959
344.3	80.58	0.6958	0.7556	0.4215	0.3242

Table III. Vapor–Liquid Equilibrium Data for the 410.9 K (137.7 °C) Isotherm of the Carbon Dioxide + *n*-Butane Binary System

T, K	P, bar	x_{CO_2}	y_{CO_2}	ρ_L, g/cm^3	ρ_V, g/cm^3
410.9	30.14	0.0000	0.0000	0.3741	0.0976
410.8	31.94	0.0113	0.0335	0.3714	0.1025
410.9	34.51	0.0291	0.0739	0.3678	0.1107
410.9	38.75	0.0575	0.1309	0.3604	0.1257
411.0	41.70	0.0774	0.1616	0.3522	0.1383
410.7	44.85	0.1009	0.1855	0.3430	0.1523
410.9	48.80	0.1333	0.2042	0.3194	0.1795
410.8	50.66	0.1529	0.2040	0.2881	0.1980
410.7	51.61	0.1739	0.2101	0.2451	0.2177

Results and Discussion

Tables I–III contain our unsmoothed, experimental data for the CO_2 + *n*-butane system at 37.7, 71.1, and 137.7 °C. Data for this system have been reported previously by Olds et al. (*3*). Figures 2 and 3 are plots of composition and density for both

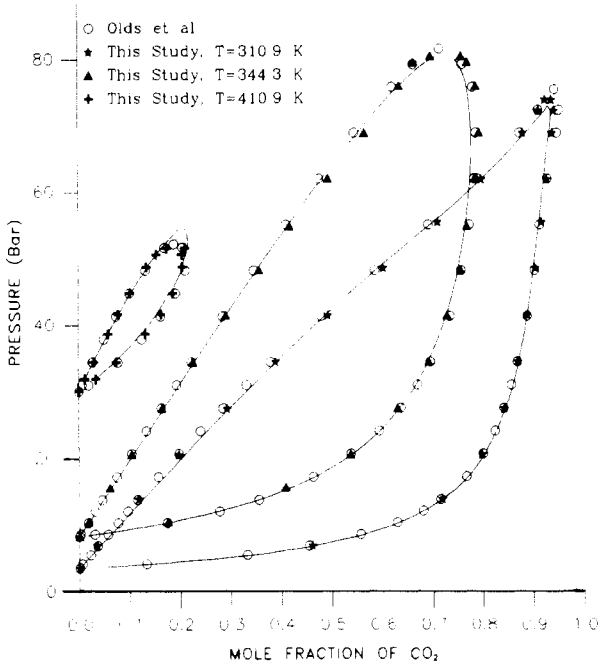

Figure 2. T–P–x–y data for carbon dioxide + n-butane. A comparison of experimental data from this study with Olds et al. (*3*) data for T = 310.9, 344.3, and 410.9 K. The data have been fit with the Peng–Robinson equation of state.

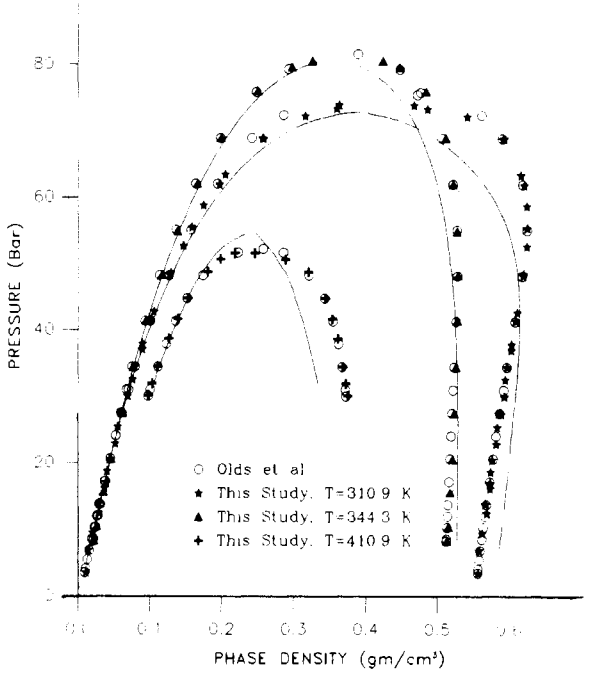

Figure 3. Phase density data for carbon dioxide + n-butane. A comparison of experimental data from this study with Olds et al. (*3*) data for T = 310.9, 344.3, and 410.9 K. The data have been fit with the Peng–Robinson equation of state.

Table IV. Vapor–Liquid Equilibrium Data for the 310.9 K (37.7 °C) Isotherm of the Nitrogen + n-Butane Binary System

T, K	P, bar	x_{N_2}	y_{N_2}	ρ_L, g/cm³	ρ_V, g/cm³
310.7	3.56	0.0000	0.0000	0.5562	0.0106
310.9	10.97	0.0121	0.6335	0.5564	0.0175
310.9	17.56	0.0239	0.7506	0.5571	0.0255
310.8	34.89	0.0532	0.8426	0.5551	0.0460
310.8	69.55	0.0988	0.8877	0.5521	0.0900
310.8	104.02	0.1540	0.9022	0.5487	0.1334
310.8	138.20	0.2115	0.8985	0.5455	0.1761
311.0	172.53	0.2894	0.8856	0.5400	0.2210
311.0	207.07	0.3530	0.8649	0.5323	0.2670
310.8	241.53	0.4268	0.8383	0.5190	0.3150
311.0	276.89	0.5431	0.7717	0.4865	0.3826
310.8	285.16	0.6103	0.7304	0.4570	0.4138

Table V. Vapor–Liquid Equilibrium Data for the 410.9 K (137.7 °C) Isotherm of the Nitrogen + n-Butane Binary System

T, K	P, bar	x_{N_2}	y_{N_2}	ρ_L, g/cm³	ρ_V, g/cm³
410.9	30.14	0.0000	0.0000	0.3741	0.0976
410.9	34.93	0.0135	0.0638	0.3689	0.1063
411.0	41.90	0.0357	0.1405	0.3600	0.1198
410.8	49.01	0.0586	0.1884	0.3517	0.1361
411.0	51.83	0.0692	0.2059	0.3459	0.1428
411.1	55.78	0.0836	0.2179	0.3363	0.1550
410.9	59.14	0.0968	0.2305	0.3296	0.1634
410.9	62.66	0.1142	0.2359	0.3180	0.1768
410.9	65.55	0.1309	0.2332	0.3031	0.1913
410.9	68.17	0.1466	0.2259	0.2844	0.2107
410.7	69.41	0.1707	0.2187	0.2718	0.2237

data sets. Agreement between our data sets and the Olds et al. data is very good.

The data for the N_2 + n-butane system are tabulated in Tables IV and V. Two isotherms, 37.7 and 137.7 °C, were measured for this system. Previously measured compositional data by Akers et al. (*4*) and Roberts and McKetta (*5*) are plotted and compared with our experimental data in Figure 4. Our density data are shown in Figure 5; there are no published density data for this system.

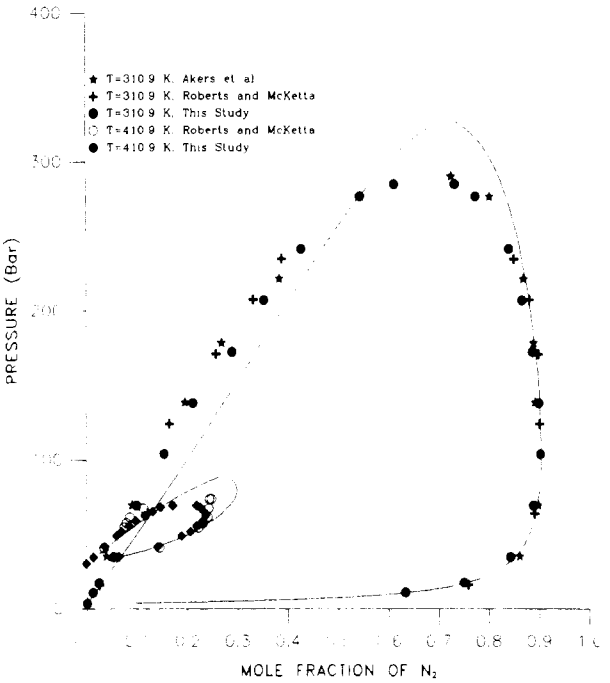

Figure 4. T–P–x–y data for nitrogen + n-butane. A comparison of experimental data from this study with Akers et al. (*4*) and Roberts and McKetta (*5*) data at T = 310.9, 344.3, and 410.9 K. The data have been fit with the Peng–Robinson equation of state.

Tables VI and VII contain our experimental, unsmoothed data for the N_2 + CO_2 + n-butane system at 37.7, 71.1, and 137.7 °C, with data taken at five pressures, 34.5, 68.9, 137.9, 206.8, and 275.7 bar, for the lower temperature, and at three pressures, 41.4, 51.7, and 62.0 bar, for the higher temperature. No data on this system have been reported previously. Figures 6–9 are composition and density plots of these data sets.

The two binary systems, CO_2 + n-butane and N_2 + n-butane, and the ternary system of N_2 + CO_2 + n-butane have all

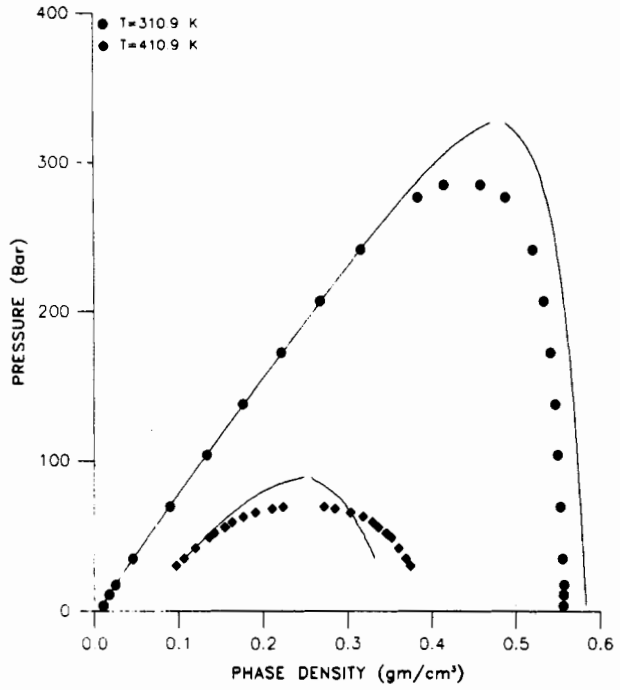

Figure 5. Phase density data for nitrogen + *n*-butane at 310.9 and 410.9 K fit with the Peng–Robinson equation of state.

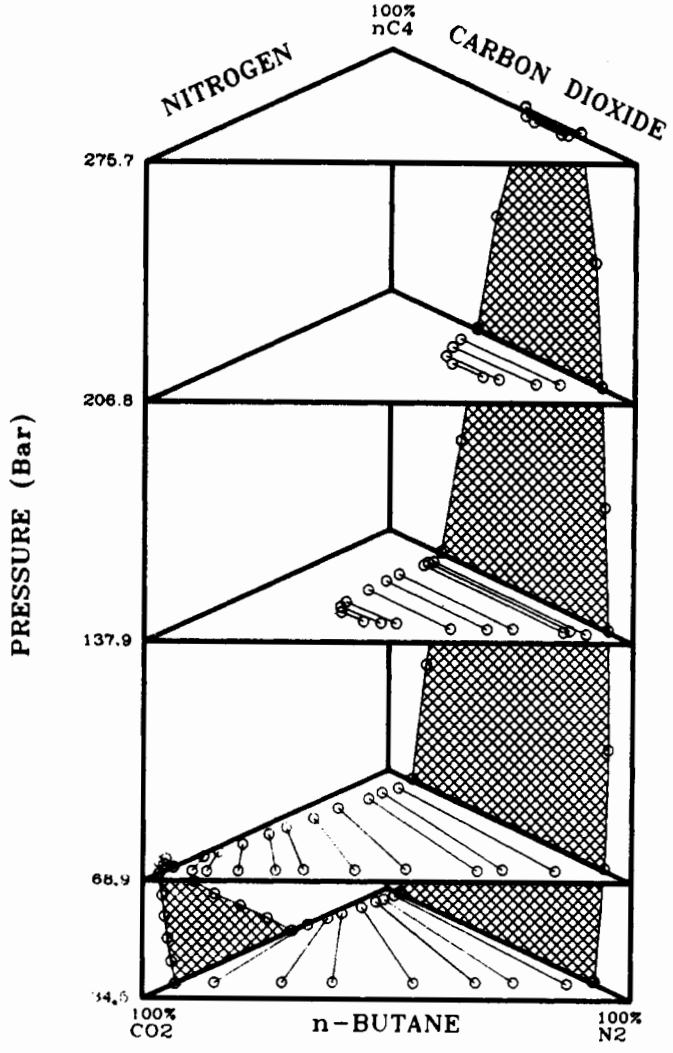

Figure 6. Phase behavior for the ternary system of nitrogen, carbon dioxide, and *n*-butane at $T = 310.9$ K and five pressures. The crosshatched areas represent the binary two-phase regions.

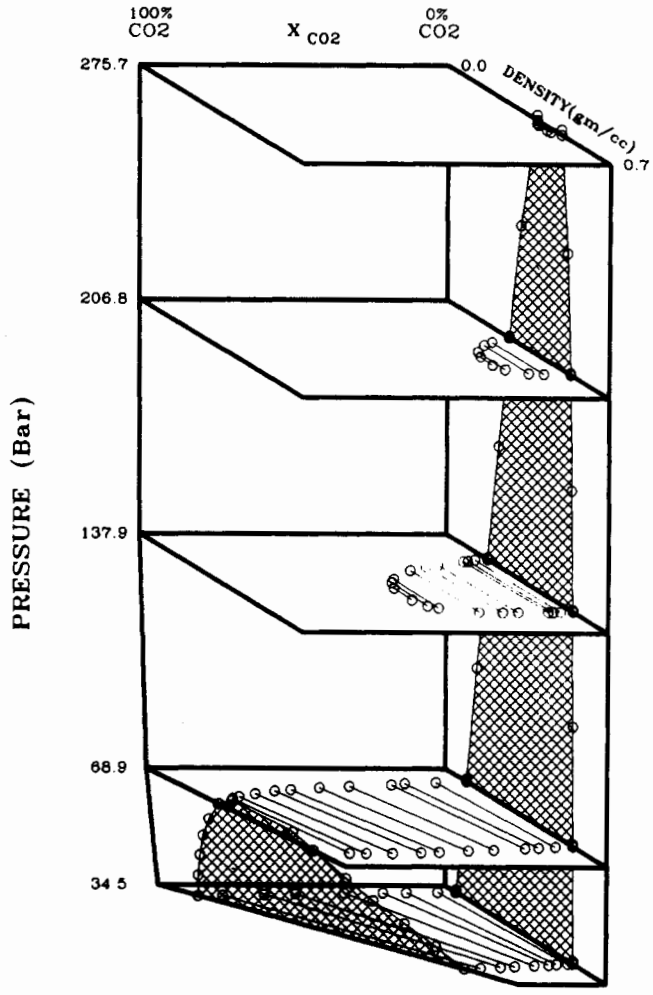

Figure 7. Three-dimensional view of phase density data for the ternary system of nitrogen, carbon dioxide, and *n*-butane at $T = 310.9$ K and five pressures. The crosshatched areas represent the binary two-phase regions.

correlated with the Peng–Robinson equation of state (EOS) (*6*) and the conventional van der Waals one-fluid mixing rules.

$$P = \frac{RT}{V - b} - \frac{a}{V(V + b) + b(V - b)} \quad (1)$$

$$a = \sum_{i=1}^{n_c}\sum_{j=1}^{n_c} x_i x_j a_{ij} \quad (2)$$

$$b = \sum_{i=1}^{n_c} x_i b_i \quad (3)$$

and

$$a_{ij} = (a_i a_j)^{1/2}(1 - k_{ij}) \quad (4)$$

The fits of the CO_2 + *n*-butane data with the Peng–Robinson EOS and van der Waals one-fluid mixing rules are shown as the solid lines in Figures 2 and 3. One adjustable interaction parameter k_{ij} fitted to the T–P–x–y data is adequate in modeling those data for this system. An isothermal flash routine was used in the fitting of the binary interaction parameter, since we perceived our error in vapor and liquid compositions to be equal at about 0.005 mole fraction. The objective function used was

$$\mathrm{OBJ} = \sum_{i=1}^{\mathrm{NPTS}}\sum_{j=1}^{\mathrm{NPTS}} (|x_j^{\mathrm{calcd}} - x_j^{\mathrm{exptl}}| + |y_i^{\mathrm{calcd}} - y_j^{\mathrm{exptl}}|) \quad (5)$$

Optimum fits of the isotherms were determined by allowing the

Table VI. Vapor-Liquid Equilibrium Data for Nitrogen + Carbon Dioxide + n-Butane Ternary System at 310.9 K (37.7 °C)

T, K	P, bar	x_{N_2}	x_{CO_2}	y_{N_2}	y_{CO_2}	ρ_L, g/cm^3	ρ_V, g/cm^3
310.8	34.89	0.0532	0.0000	0.8426	0.0000	0.5551	0.0460
310.8	34.59	0.0486	0.0194	0.7959	0.0610	0.5571	0.0487
310.9	34.54	0.0447	0.0577	0.6808	0.1648	0.5601	0.0503
310.9	34.58	0.0407	0.0858	0.6051	0.2434	0.5638	0.0536
311.2	34.40	0.0329	0.1368	0.4790	0.3709	0.5684	0.0563
310.7	34.52	0.0234	0.2074	0.3153	0.5359	0.5766	0.0628
310.6	34.46	0.0166	0.2577	0.2123	0.6414	0.5819	0.0668
311.0	34.62	0.0067	0.3300	0.0770	0.7844	0.5913	0.0757
310.9	34.53	0.0000	0.3878	0.0000	0.8679	0.5962	0.0788
310.8	69.55	0.0988	0.0000	0.8877	0.0000	0.5521	0.0900
310.9	69.00	0.1035	0.0612	0.7900	0.1056	0.5579	0.0976
311.0	69.28	0.0963	0.1205	0.6819	0.2130	0.5636	0.1050
310.8	68.86	0.0900	0.1684	0.6311	0.2639	0.5675	0.1146
310.8	69.28	0.0781	0.2801	0.4843	0.4090	0.5785	0.1262
311.0	69.00	0.0684	0.3697	0.3821	0.5148	0.5875	0.1368
310.8	69.14	0.0571	0.4710	0.2792	0.6213	0.5965	0.1542
310.9	69.00	0.0487	0.5345	0.2233	0.6804	0.6013	0.1625
310.9	68.86	0.0377	0.6317	0.1483	0.7595	0.6070	0.1824
310.9	69.14	0.0261	0.7176	0.0892	0.8285	0.6080	0.2040
310.8	69.28	0.0192	0.7708	0.0604	0.8603	0.6063	0.2182
310.8	68.93	0.0000	0.8772	0.0000	0.9351	0.5902	0.2552
310.8	138.20	0.2115	0.0000	0.8985	0.0000	0.5455	0.1761
310.8	137.24	0.2225	0.0423	0.8519	0.0463	0.5479	0.1824
311.1	137.93	0.2267	0.0677	0.8146	0.0756	0.5505	0.1911
310.7	137.65	0.2233	0.0834	0.8035	0.0919	0.5495	0.1929
310.9	138.34	0.2244	0.1840	0.6976	0.1925	0.5535	0.2178
310.9	138.07	0.2236	0.2356	0.6430	0.2431	0.5541	0.2314
310.9	137.93	0.2257	0.3112	0.5642	0.3130	0.5529	0.2577
310.9	138.76	0.2465	0.4224	0.4431	0.4132	0.5248	0.3195
310.8	138.34	0.2510	0.4483	0.4050	0.4380	0.5113	0.3441
310.9	138.07	0.2729	0.4665	0.3573	0.4614	0.4684	0.3847
311.0	207.07	0.3530	0.0000	0.8649	0.0000	0.5323	0.2670
310.8	207.41	0.3694	0.0846	0.7719	0.0808	0.5274	0.2989
310.8	207.14	0.3830	0.1310	0.7168	0.1242	0.5236	0.3218
310.8	207.27	0.4130	0.1865	0.6226	0.1808	0.4950	0.3700
311.0	207.00	0.4539	0.2040	0.5753	0.1990	0.4636	0.4048
311.0	276.89	0.5431	0.0000	0.7717	0.0000	0.4865	0.3826
310.8	275.65	0.5639	0.0184	0.7353	0.0177	0.4650	0.4023
310.9	275.31	0.6018	0.0226	0.7121	0.0220	0.4527	0.4147

Table VII. Vapor-Liquid Equilibrium Data for Nitrogen + Carbon Dioxide + n-Butane Ternary System at 410.9 K (137.7 °C)

T, K	P, bar	x_{N_2}	x_{CO_2}	y_{N_2}	y_{CO_2}	ρ_L, g/cm^3	ρ_V, g/cm^3
411.0	41.90	0.0357	0.0000	0.1405	0.0000	0.3600	0.1198
410.8	41.69	0.0304	0.0119	0.1136	0.0272	0.3593	0.1220
410.9	41.43	0.0163	0.0412	0.0613	0.0902	0.3560	0.1283
410.9	41.42	0.0052	0.0658	0.0190	0.1390	0.3528	0.1350
411.0	41.70	0.0000	0.0774	0.0000	0.1616	0.3522	0.1383
411.0	51.83	0.0692	0.0000	0.2059	0.0000	0.3459	0.1428
411.0	51.74	0.0615	0.0210	0.1697	0.0390	0.3424	0.1484
411.0	51.80	0.0542	0.0354	0.1461	0.0631	0.3398	0.1541
410.8	51.70	0.0479	0.0538	0.1218	0.0945	0.3372	0.1581
410.8	52.10	0.0285	0.1017	0.0591	0.1578	0.3220	0.1781
410.8	52.12	0.0232	0.1153	0.0458	0.1706	0.3126	0.1868
410.8	51.82	0.0077	0.1511	0.0127	0.1993	0.2915	0.2048
410.7	51.62	0.0000	0.1739	0.0000	0.2101	0.2451	0.2177
410.9	62.66	0.1142	0.0000	0.2359	0.0000	0.3180	0.1768
411.0	62.52	0.1109	0.0044	0.2299	0.0067	0.3186	0.1770
411.0	62.11	0.0980	0.0391	0.1757	0.0536	0.2990	0.1952
410.8	62.24	0.0972	0.0519	0.1579	0.0689	0.2897	0.2037
410.8	62.24	0.0956	0.0705	0.1310	0.0839	0.2702	0.2244

k_{ij} parameter to be temperature dependent (Table VIII). Predictions of the CO_2 + n-butane phase density data using the k_{ij} determined from fitting the $T-P-x-y$ data are less satisfactory. The differences between the experimental data and the calculated results are most noticeable in the liquid densities and densities near the mixture critical point of each isotherm. [Note that the phase densities were not used in fitting the binary interaction parameter, nor would including them have improved the fit significantly.] Table VIII contains the binary interaction parameters determined and used in this work.

The fits of the N_2 + n-butane data with the Peng-Robinson EOS and van der Waals one-fluid mixing rules are shown in Figures 4 and 5. These fits are generally poor with large overpredictions of the mixture critical point. No adustment of the binary interaction parameters improved the fit of these isotherms. Predictions of the liquid densities and mixture critical densities are also poor. In a subsequent paper, we will discuss modeling techniques to reduce this overprediction of the critical points and improve the density predictions. It is worth noting that Knapp et al. have observed similar behavior for other N_2 + hydrocarbon systems (7).

The accuracy of the composition predictions for the ternary experimental data depends on the fit of the binary systems which form the boundaries of the ternary system (i.e., the N_2

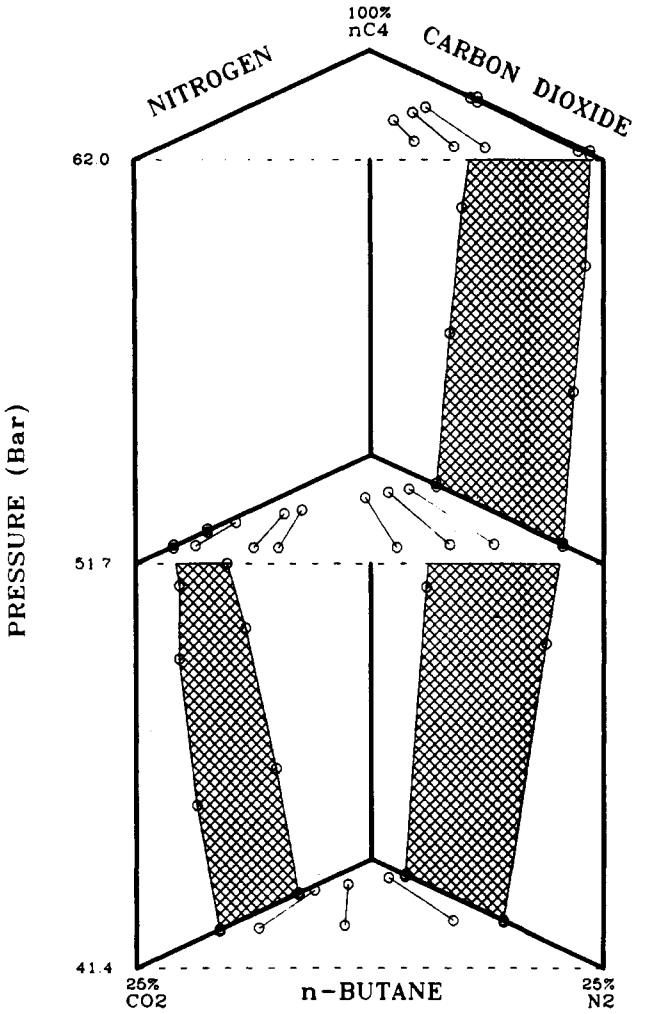

Figure 8. Phase behavior for the ternary system of nitrogen, carbon dioxide, and *n*-butane at T = 410.9 K and three pressures. The crosshatched areas represent the binary two-phase regions.

Table VIII. Binary Interaction Parameters for the Peng-Robinson Equation of State

Carbon Dioxide + *n*-Butane Binary System	
T = 310.9 K	k_{CO_2+nC4} = 0.117
T = 344.3 K	k_{CO_2+nC4} = 0.126
T = 410.9 K	k_{CO_2+nC4} = 0.197
Nitrogen + *n*-Butane Binary System	
T = 310.9 K	k_{N_2+nC4} = 0.000
T = 410.9 K	k_{N_2+nC4} = 0.128
Nitrogen + Carbon Dioxide + *n*-Butane Ternary System	
T = 310.9 K	k_{CO_2+nC4} = 0.117
	k_{N_2+nC4} = 0.000
	$k_{CO_2+N_2}$ = 0.000
T = 410.9 K	k_{CO_2+nC4} = 0.197
	k_{N_2+nC4} = 0.128
	$k_{CO_2+N_2}$ = 0.000

+ *n*-butane, CO_2 + *n*-butane, and N_2 + CO_2 systems). The quality of the fit of the N_2 + *n*-butane and CO_2 + *n*-butane systems largely determined the quality of the ternary predictions since the interaction parameter for the N_2 + CO_2 system is approximately zero (*7*) at all measured temperatures. This trend can be seen in Figures 10 and 11, which are representative of the other fits. In Figure 10, both the N_2 + *n*-butane and CO_2 + *n*-butane binary systems were fit well at pressure and temperature of the experiments and this is reflected in the quality of the ternary predictions. In Figure 11, the CO_2 + *n*-butane binary system is fit well, but the N_2+ *n*-butane binary fit is poor and so are the predictions for the ternary system.

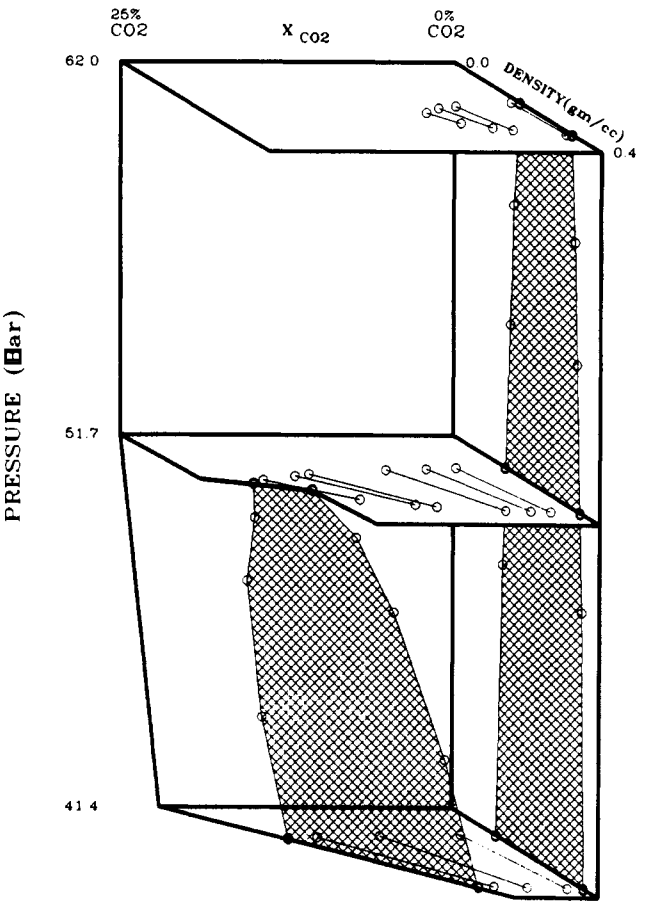

Figure 9. Three-dimensional view of phase density data for the ternary system of nitrogen, carbon dioxide, and *n*-butane at T = 410.9 K and three pressures. The crosshatched areas represent the binary two-phase regions.

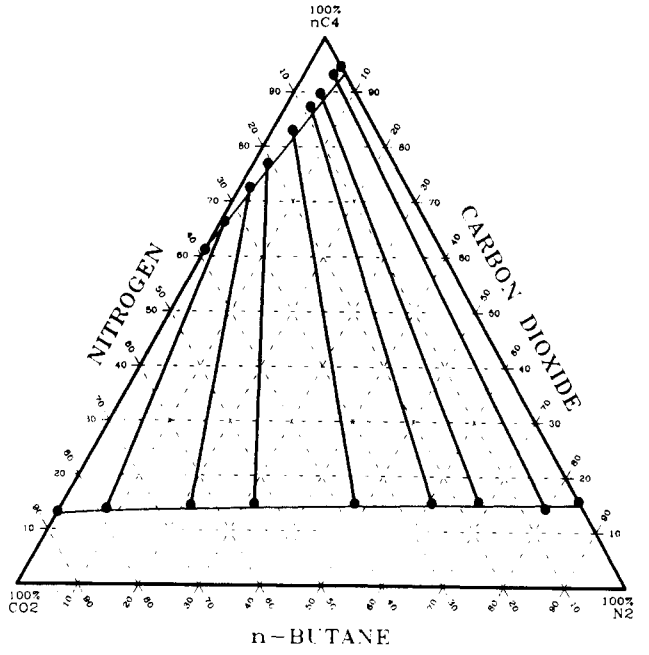

Figure 10. Phase diagram for the ternary mixture of nitrogen, carbon dioxide, and *n*-butane, at T = 310.9 K and P = 34.5 bar (500 psia) fit with the Peng–Robinson equation of state.

It should be noted that the values of the interaction parameters used in the ternary mixture calculations were obtained only from analysis of the binary systems. The predictions of the ternary data involved no adjustment of the binary interaction parameters.

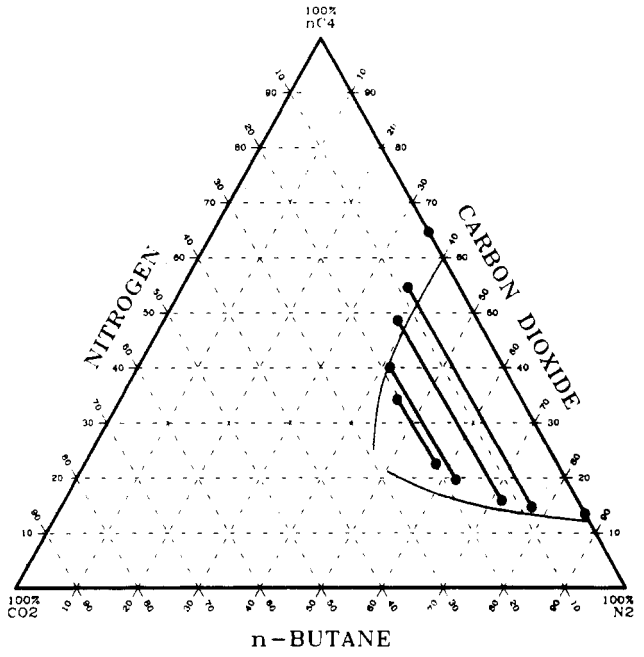

Figure 11. Phase diagram for the ternary mixture of nitrogen, carbon dioxide, and *n*-butane, at T = 310.9 K and P = 206.8 bar (3000 psia) fit with the Peng-Robinson equation of state.

Conclusions

A new, high-pressure vapor-liquid equilibrium apparatus capable of measuring the compositions and densities of the coexisting phases up to 300 °F and 5000 psia has been built, tested, and used to obtain data for the CO_2 + *n*-butane, N_2 + *n*-butane, and N_2 + CO_2 + *n*-butane systems. Data for the first of these systems are in excellent agreement with previously published data for both compositions and densities. The compositional data for the CO_2 + *n*-butane system were fit well with the Peng-Robinson equation of state with van der Waals one-fluid mixing rules, though (as is expected) the liquid density predictions were poor. Both the compositions and densities of the N_2 + *n*-butane system are poorly fit in this way, as is typical of N_2-hydrocarbon systems. Since the constituent binary systems were poorly fit with the Peng-Robinson equation of state, so was the data for the ternary N_2 + CO_2 + *n*-butane system.

Registry No. N_2, 7727-37-9; CO_2, 124-38-9; butane, 106-97-8.

Literature Cited

(1) Behrens, P. K.; Sandler, S. I. *J. Chem. Eng. Data* **1983**, *28*, 52.
(2) Eckert, C. J.; Sandler, S. I. *J. Chem. Eng. Data* **1986**, *31*, 26.
(3) Olds, R. H.; Reamer, H. H.; Sage, B. H.; Lacey, W. N. *Ind. Eng. Chem.* **1947**, *41*, 475.
(4) Akers, W. W.; Attwell, L. L.; Robinson, J. A. *Ind. Eng. Chem.* **1954**, *46*, 2539.
(5) Roberts, L. R.; McKetta, J. J. *AIChE. J.* **1961**, *7*, 173.
(6) Peng, D.-Y.; Robinson, D. B. *Ind. Eng. Chem. Fundam.* **1976**, *15*, 59.
(7) Knapp, H.; et al. *Vapor-Liquid Equilibria For Mixtures of Low Boiling Substances*; DECHEMA Chemistry Data Series VI; DECHEMA: Frankfurt/Main, West Germany, 1982.

Received for review July 25, 1988. Accepted March 30, 1989. This work was supported, in part, by Grant CBT-8812285 from the National Science Foundation to the University of Delaware and a grant from the Chevron Oil Field Research Company.

Vapor–Liquid Equilibria at 760 mmHg in the Ternary System Methyl Acetate–Propyl Bromide–Toluene

Jaime Wisniak* and Abraham Tamir

Department of Chemical Engineering, Ben Gurion University of the Negev, Beer-Sheva, Israel 84105

Vapor–liquid equilibria at atmospheric pressure have been determined for the title ternary system. The data were correlated by various equations, and the appropriate parameters are reported.

The present work was undertaken to measure VLE data for the ternary system methyl acetate–propyl bromide–toluene for which no isobaric data are available. Data for the pertinent binaries have been reported previously (*1*, *2*).

Experimental Section

Purity of Materials. Methyl acetate (99.2+%) and propyl bromide (99.4+%) were purchased from Merck, and toluene (99.6+%) was purchased from Frutarom. The reagents were used without further purification after gas chromatography failed to show any significant impurities. Properties of the pure components appear in Table I.

Table I. Physical Constants of Pure Components

index	compd	refract. index at 25 °C	bp(760 mmHg), °C	purity GLC (min)
1	methyl acetate	1.3588[a]	56.94[a]	99.2
		1.3589[b]	56.94[b]	
2	propyl bromide	1.4320[a]	70.55[a]	99.4
		1.4317[b]	70.80[b]	
3	toluene	1.4926[a]	110.70[a]	99.6
		1.4941[b]	110.63[b]	

[a] Measured. [b] Reference *10*.

Apparatus and Procedure. An all-glass modified Dvorak and Boublik recirculation still (*3*) was used in the equilibrium determination. The experimental features have been described in previous publications (*4*). All analyses were carried out by gas chromatography on a Packard-Becker Model 417 apparatus provided with a thermal conductivity detector and an Autolab Model 6300 electronic integrator. The column was 200 cm long and 0.2 cm in diameter, was packed with OV-17 20%, and

* To whom correspondence should be addressed.

0021-9568/89/1734-0298$01.50/0